MISSOURI
S&T

Missouri University of Science and Technology

Scholars' Mine

International Conferences on Recent Advances in Geotechnical Earthquake Engineering and Soil Dynamics

1991 - Second International Conference on Recent Advances in Geotechnical Earthquake Engineering & Soil Dynamics

12 Mar 1991, 2:30 pm - 3:30 pm

Experimental Study on Lateral Flow of Ground Due to Soil Liquefaction

Yasushi Sasaki
Ministry of Construction, Japan

Hideo Matsumoto
Ministry of Construction, Japan

Ken-ichi Tokida
Ministry of Construction, Japan

Syoichi Saya
Ministry of Construction, Japan

Follow this and additional works at: https://scholarsmine.mst.edu/icrageesd

Part of the Geotechnical Engineering Commons

Recommended Citation

Experimental Study on Lateral Flow of Ground Due to Soil Liquefaction

Yasushi Sasaki, Director, Earthquake Disaster Prevention Department, Public Works Research Institute, Ministry of Construction, Japan

Ken-ichi Tokida, Head, Ground Vibration Division, Earthquake Disaster Prevention Department, Public Works Research Institute, Ministry of Construction, Japan

Hideo Matsumoto, Research Engineer, Earthquake Disaster Prevention Department, Public Works Research Institute, Ministry of Construction, Japan

Syoichi Saya, Assistant Research Engineer, Earthquake Disaster Prevention Department, Public Works Research Institute, Ministry of Construction, Japan

SYNOPSIS: A series of shake table tests is carried out on the lateral flow of the ground due to soil liquefaction during earthquakes. The model grounds are 6.0 m long, 0.8 m wide and their average height is 1.2 m. The slope of the ground surface and the lower boundary condition of liquefiable layer are varied, and the sinusoidal accelerations with a frequency of 2 Hz are inputted for 20 seconds. The deformation of model grounds, the excess pore water pressure of the liquefied layer, and the acceleration of the grounds are monitored. Based on the test results, the influence of the slope, the input motion and the thickness of liquefied layer to the ground flow is examined, and the fundamental characteristics of lateral ground flow induced by soil liquefaction are clarified experimentally.

INTRODUCTION

The liquefaction has caused severe damages for structures during the past earthquakes in Japan. Hamada et. al. (1986,1988) pointed out that the fairly big amount of lateral flow of ground could be seen broadly at the areas in and/or around Tokyo, Fukui, Niigata and Noshiro where the liquefaction of the ground apparently took place during the Kanto Earthquake (1923, M=7.9), the Fukui Earthquake (1948,M=7.3) the Niigata Earthquake (1964, M=7.5) and the Nihonkai-chubu Earthquake (1983, M=7.7), respectively. Therefore it becomes necessary to consider two types of effect induced by soil liquefaction for the earthquake resistant design of structures; the loss of bearing capacity of liquefied ground and the lateral flow of the inclined ground induced by liquefaction. The loss of bearing capacity of liquefied layers has been considered in the "Specifications for Highway Bridges" (1980, 1990) in Japan. However, the mechanism of ground flow induced by soil liquefaction, the predicting method of ground flow and the applying method of its effect to the earthquake resistant design of structures are not yet clarified at present. Under these circumstances, as the first stage of investigations, the authors conduct a series of shake table tests to study the mechanism of ground flow induced by soil liquefaction and to establish the procedure for estimating ground flow. This paper describes the essential factors relating to the lateral ground flow due to soil liquefaction explained from the experiments.

METHOD OF EXPERIMENTS

Shake table tests on eight model grounds (Model-1 ~ 8) are carried out. The conditions of ground models are shown in Fig. 1 and Table 1. The two types of containers placed on a shake table are prepared to set up model grounds: a square container for Model-1 ~ 7 is 6.0 m long, 0.8 m wide and 2.0 m high, and another semicircular one for Model-8 is 4.0 m long with a diameter and 0.4 m high. Four transparent glass windows (each is 0.8 m wide

Table 1 Characteristics of Ground Models

Model No.	Slope of Surface θ_s (%)	Slope of Lower Boundary of Liquefiable Layer θ_b (%)	Thickhess of Liquefiable Layer H_L (cm)	Liquefiable Layer Unit Weight γ_{t1} (tf/m³)	Unsaturated Surface Layer		
					Unit Weight γ_{t2} (tf/m³)	Materials	
1	5	0	7 0	1. 9 3	1. 4 9	sand	
2	7. 5	0	3 5	1. 8 8	1. 3 7	sand	
3	5	5	5 ~ 3 5	1. 9 3	1. 5 7	sand	
4	5	0	3 5	1. 9 0	1. 4 9	sand	
5	2. 5	0	3 5	2. 0 6	5. 7 1	shot of lead	
6	0 ~ 5	0	3 5	2. 0 0	1. 4 8	gravel	
7	0	5	3 5 ~ 6 5	1. 9 3	———	———	
8	1 5	0	2 5	1. 8 4	1. 3 6	gravel	

and 1.8 m high) are installed at the one side of the square container. Models-1 ~ 7 are prepared as a two-dimensional ground model to investigate the influence of the ground conditions on the lateral ground flow, and on the other hand, Model-8 is prepared as a three-dimensional ground model to know the influence of the direction of excitation on the lateral ground flow. The model grounds fundamentally consist of three layers: a lowermost nonliquefiable layer, a middle liquefiable layer and a uppermost unsaturated layer. However, Models-7 and 8 do not have the uppermost unsaturated layer and the lowermost nonliquefiable layer, respectively. The materials used for model grounds are shown in Table 2, i.e., mountain sand taken from Mt. Sengen-yama for three layers and shot of lead or gravel for the uppermost layer.

As for preparation of the model grounds, the lowermost sand layer is firstly compacted enough in the container not to liquefy during excitation, a certain amount of water is poured, and then the middle liquefiable sand layer is prepared by means of the underwater drop method. Upon completion of the lowermost and middle layers, the uppermost unsaturated layer is prepared forming the surface ground with a slope. In the Models-5, 6 and 8, shot of lead or gravel is used as the material of the unsaturated layer to give the larger overburden pressure and lesser · cohesion than Mt. Sengen-yama Sand. Based on Table 2 as for the unit weight of unsaturated surface layer, the unit weight of gravel is not so different from that of Mt. Sengen-yama Sand, but the unit weight of shot of lead is about four times than that of Sand. The thickness of liquefiable layer (H_1), the slopes of surface (θ_s) and lower boundary of liquefiable layer (θ_b) are varied to have different conditions in order to examine the influence of these factors on the ground flow. The water level is set equal to the upper boundary of liquefiable layer, i.e., horizontal regardless of the slope of ground surface in this series of tests.

The typical conditions of each model ground are indicated as follows:

Table 2 Characteristics of Ground Materials

1) Sand (Mt. Sengen-yama Sand)

Specific Gravity of Soil Particle G_s	2. 6 5 5
Maximum Void Ratio e_{max}	0. 9 7 6
Minimum Void Ratio e_{min}	0. 5 9 6
Maximum Grain Size (mm)	4. 7 6
Mean Grain Size D_{50}(mm)	0. 2 7
Coefficient of Uniformity U_c	1. 3 7

2) Shot of Lead

Specific Gravity of Soil Particle G_s	1 1. 3 4
Mean Grain Size D_{50}(mm)	2. 0 0

3) Gravel

Maximum Grain Size (mm)	9. 5 2

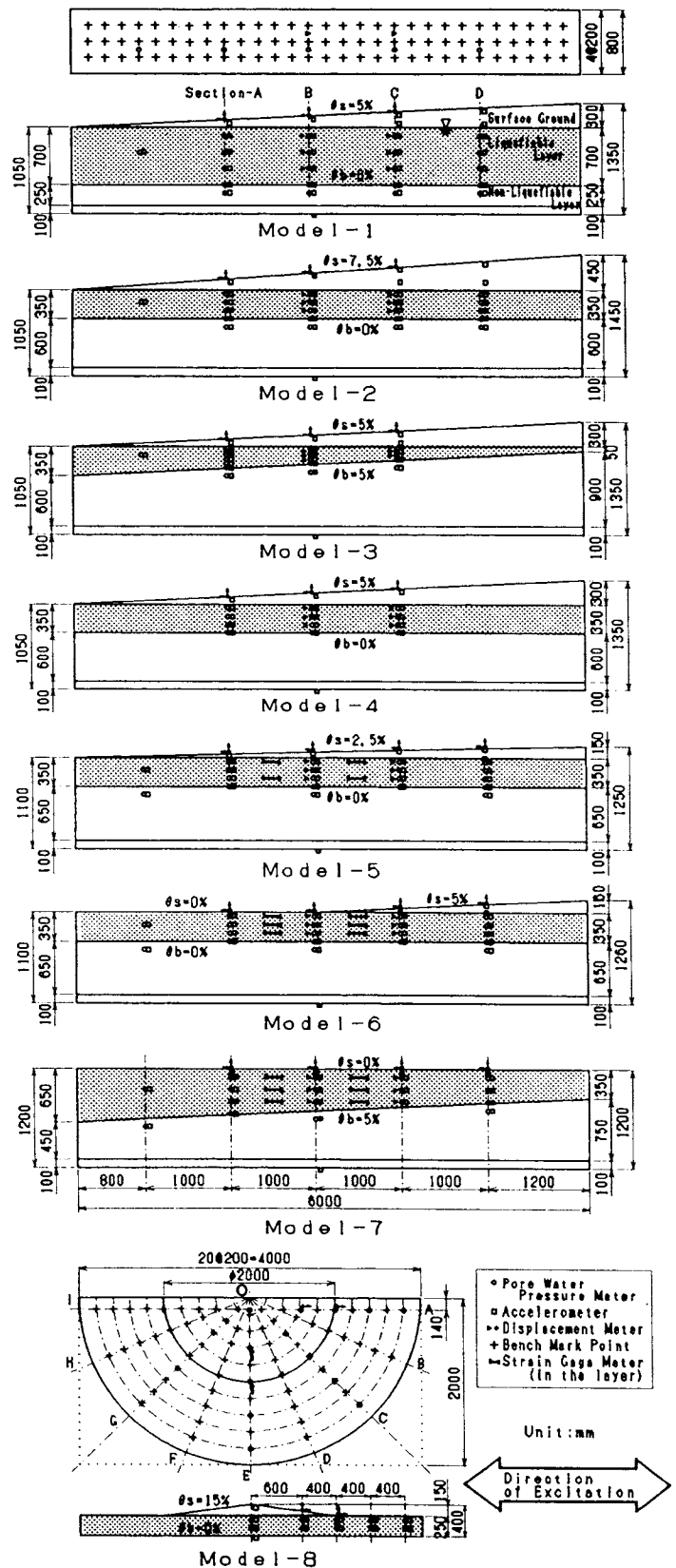

Fig. 1 Ground Models and Measurements

Model-1: θ_s= 5 %, θ_b= 0 % and H_1= 700 mm.
   H_1 is larger than Model-4 (H_1= 350mm).
Model-2: θ_s=7.5 %, θ_b= 0 % and H_1= 350 mm.
   θ_s is larger than Model-4 (θ_s=5.0%).
Model-3: θ_s= 5 %, θ_b= 5 % and H_1= 350 ~ 50 mm.
   The lower boundary of liquefiable layer
   inclines comparing with Model-4 (θ_b= 0
   %).
Model-4: θ_s= 5 %, θ_b= 0 % and H_1= 350 mm.
Model-5: θ_s=2.5 %, θ_b= 0 % and H_1= 350 mm.
   The slope of shot of lead (converted
   into about θ_s= 10 % as sand) is larger
   than Model-4(θ_s= 5 %) and Model-2(θ_s
   = 7.5 %)
Model-6: θ_s= 0, 5 %, θ_b= 0 % and H_1= 350 mm.
   The ground surface is inclined and
   horizontal.
Model-7: θ_s= 0 %, θ_b= 5 % and H_1= 650 ~ 350mm.
   Only lower boundary of liquefiable layer
   is inclined.
Model-8: θ_s= 15 %, θ_b= 0 % and H_1= 250 mm.
   The surface ground shapes a semi-corn
   with gravel.
In each test, constant sinusoidal acceleration
with a frequency of 2 Hz is employed for 20
seconds (40 cycles), and several levels of
maximum acceleration (60 ~ 190 gals) are applied
stepwise to the shake table as input motion.
The measured maximum accelerations of the shake
table and the results of typical lateral
displacement on the ground surface at Section-B
are summarized in Table 3 for all tests.
As shown in Fig. 1, accelerometers, pore water
pressure meters, strain gage meters and
displacement meters are installed in or on the

Table 3 Input Motion and Lateral Displacement

Model No.	Shaking Step No.	Maximum Acceleration at Table α_{max}(gal)	Lateral Displacement at Surface (Section B)(mm)
1	1	80	61
	2	110	169
	3	160	118
	4	220	56
2	1	65	28
	2	110	144
	3	155	165
	4	105	62
3	1	65	68
	2	110	156
	3	90	87
	4	85	35
4	1	65	6
	2	95	72
	3	140	142
	4	190	44
5	1	60	1
	2	101	4
	3	152	210
	4	154	69
6	1	60	1
	2	104	101
	3	153	106
	4	154	54
7	1	64	-2
	2	103	17
	3	154	11
	4	151	6
8	1	51	14
	2	94	11
	3	95	5

ground models to measure the time history of
acceleration, pore water pressure and
displacement of layers during excitation. As
shown in Fig. 1, these meters are installed at
four sections, i.e., Sections-A,B,C and D for
Models-1 ~ 7, and at two sections, i.e.,
Section-OA (direction of excitation) and
Section-OE (right-angle direction of excitation)
for Model-8. Vertical marked lines with a
white-colored sand are also installed behind the
transparent glass windows at intervals of 20 cm
for Models-1 ~ 7 to trace or photograph the
deformation of the layers in the direction of
depth. Bench mark points are also set on the
ground surface to measure manually or photograph
the change of lateral displacement of ground
surface.

RESULTS OF EXPERIMENTS

From the above shake table tests, principal
characteristics of lateral ground flow due to
liquefaction and factors concerning to the
ground flow are drawn as follows.

Distribution of Ground Flow

Photos. 1(a) and 1(b) shows the deformation of
model ground by the vertical marked lines
through the four transparent glass windows at
the Step-2 in the case of Model-4, comparing
before excitation with after one. It can be
seen that the model ground is deformed in the
direction of slope (left side of Photos.) due to
excitation.
Figs. 2(a) and 2(b) show the successive change
of vertical marked lines during excitation at
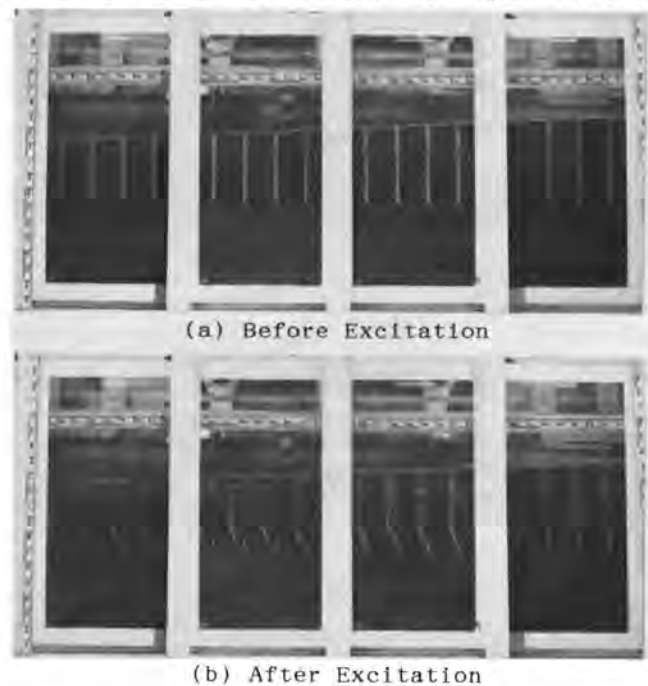the Step-2 in the cases of Models-4 and 6,

(a) Before Excitation

(b) After Excitation

Photo. 1 Ground Flow due to Liquefaction
(Model-4, Step-2)

(a) Model-2 (Step-2; α_{max}=110gal)

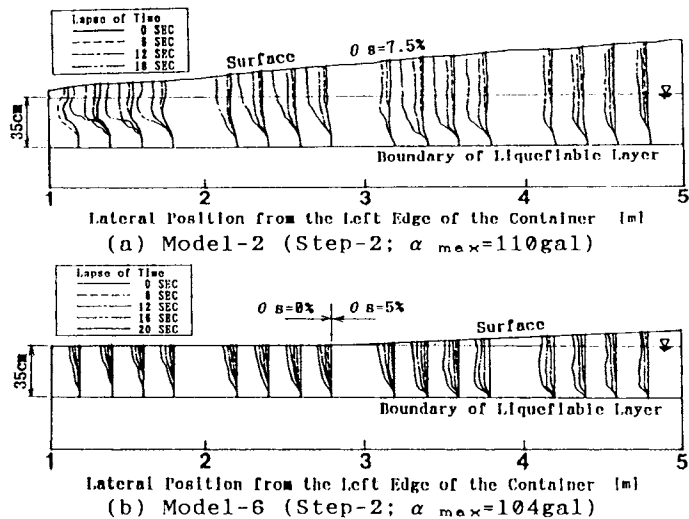(b) Model-6 (Step-2; α_{max}=104gal)

Fig. 2 Time-history of Lateral Deformation

respectively. These figures are drawn from photographs taken through the four transparent glass windows which is 4.0 m long on the side of the container. Based on these figures, it can be noted that the lateral displacement of the model ground increase gradually in the direction of slope according to the lapse of exciting time, and the unsaturated surface layer seems to deform uniformly in the direction of depth, i.e., the deformations of surface layers are not induced by the deformation of itself but by the deformation of the liquefied layer. Because the lowermost nonliquefied layer is not deformed, the displacement at the lower boundary of the middle liquefied layer is almost zero, and the lateral displacement increases upwards in the liquefied layer. The shape of deformation of liquefied layers seems to be different according to the position of the section and the lapse of exciting time. In the case of Model-6, the horizontal ground neighboring with the inclined surface ground is deformed laterally by the flow of slope, but the deformation decreases far away from the boundary of the slope.

Fig. 3 shows the typical distribution of lateral displacement and strain at the surface in the case of Models-4 and 6. The lateral displacements are estimated by measuring the positions of bench marked points set on the ground surface after each step of excitation, and indicate the magnitude of lateral movement in the direction of slope. The lateral strains are calculated based on the relative displacement and the distance of two bench marked points, and the tensile and compressive strains indicate the spread and shrink of the surface ground, respectively. In the case of Model-4, the middle sand layer doesn't liquefy and the ground flow doesn't occur at the Step-1, but the ground displacements increase according to the increase of input accelerations. Because the displacements are largest in the middle of slope, the tensile strains occur at the upper-side of slope, and on the other hand, the

compressive strains occur at the lower-side of one. In the case of Model-6, the displacements are largest at the middle of slope, the tensile strains occur at the slope and the compressive strains occur at the horizontal ground.

Relation between Acceleration, Excess Pore Water Pressure and Ground Flow During Excitation

Fig. 4 shows the typical relation of time histories between input motion, ground acceleration, excess pore water pressure in the liquefied layer and lateral displacement on the surface for Section-A at the Step-2 in the case of Model-6. From this result, it can be seen that the acceleration in the liquefiable layer seems to increase according to increase of excess pore water pressure and becomes maximum just before the excessive pore water pressure approaches to the effective overburden pressure, and decreases to zero gradually after the sand layer liquefies almost perfectly. On the other hand, the lateral displacement of the surface seems to begin to increase just before the excess pore water pressure increase to maximum,

(a) Model-4 (θ_s=5%, θ_b=0%, H_1=350mm)

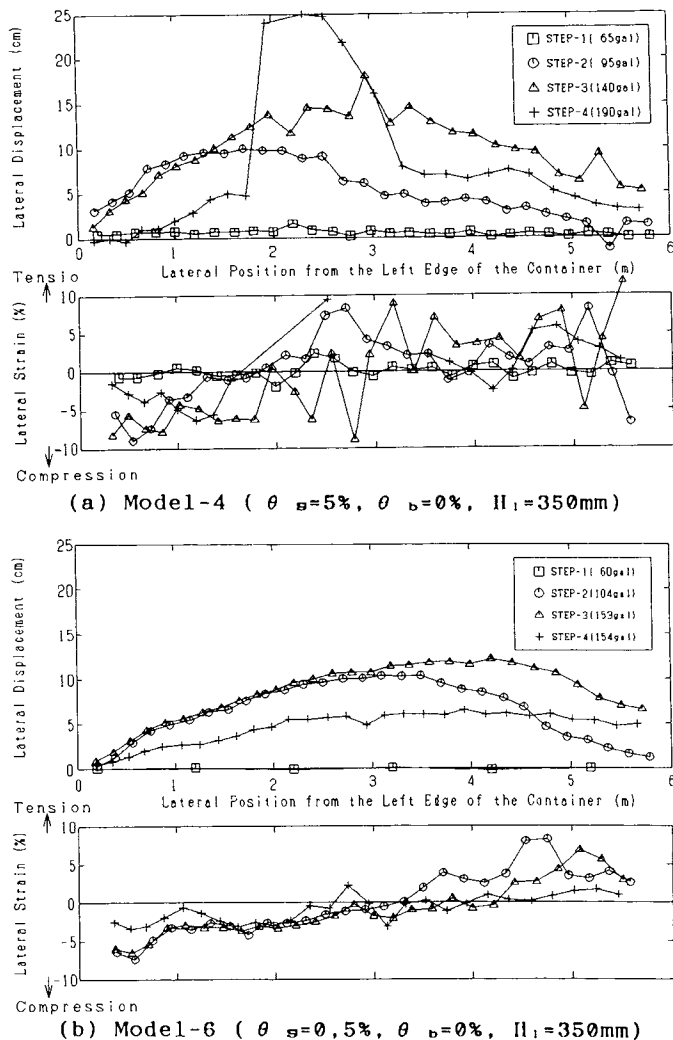(b) Model-6 (θ_s=0,5%, θ_b=0%, H_1=350mm)

Fig. 3 Lateral Deformation of Ground Surface

and continue to increase according to the lapse of exciting time.

Fig. 5 shows the relation of time history between the lateral displacement at four points on the surface and the excess pore water pressure in liquefied layer at Section A, B, C and D. From these figures, the displacement on the ground surface also can be seen to begin to increase suddenly just after the excess pore water pressure ratio ($\Delta u / \sigma'_v$) approaches to the range of 0.8 to 1.0, and also continue to increase gradually during excitation after the complete liquefaction.

Behavior of Ground after Excitation

Fig. 4 also shows the behavior after stopping excitation. After excitation, the excess pore water pressure seems to keep the high pressure constantly by seepage pressure for about 2 minutes, and it takes more than 10 minutes for high excess pore water pressure to decrease to almost zero. On the other hand, the displacement on the ground surface increases a little after excitation, but it seems very small comparing with that during excitation. From the site observation on the liquefaction and lateral ground flow in the past earthquakes, sand boils, water springs and ground movements are reported to continue for a while after the earthquake.

However the water spring can be observed at the ground surface for a while after excitation in this experiments, the progress of lateral deformation of ground can't be observed. The cause of the difference on ground flow induced by liquefaction between the actual phenomena at sites during earthquakes and the experiments can not be cleared at present.

Relation between Input Motion and Direction of Ground Flow

Fig. 6(a) shows the direction and quantity of displacement of the bench mark points which are set on the radial lines (Section-OA ~ Section-OI) at the ground surface at the Step-2 in the case of Model-8, comparing the direction of ground flow with that of excitation. From this figure, the surface of the semi-corn shaped slope and the neighboring horizontal ground seem to move almost radially, that is, in the direction of slope. Fig. 6(b) shows the distribution of displacement in the direction of slope for each Section, i.e., the vertical and lateral axes indicate the distance from the center of semi-circle in Fig. 6(a) and the position of Sections in the direction of circumference, respectively, and the shadowed area means the quantity of displacement in the direction of slope. As shown in Fig. 6(b), the displacement of surface ground in the direction of slope seems almost uniformly, except for the Sections neighboring the container which may be affected by the friction of the side wall.

Figs. 7(a) and 7(b) show the relation of time histories between excess pore water pressure (Δu) in the liquefied layer and the lateral

displacement (D) at the middle of surface of semi-corn, comparing the meters set at the Section-OA in the direction of excitation with the one set at the Section-OE in the direction
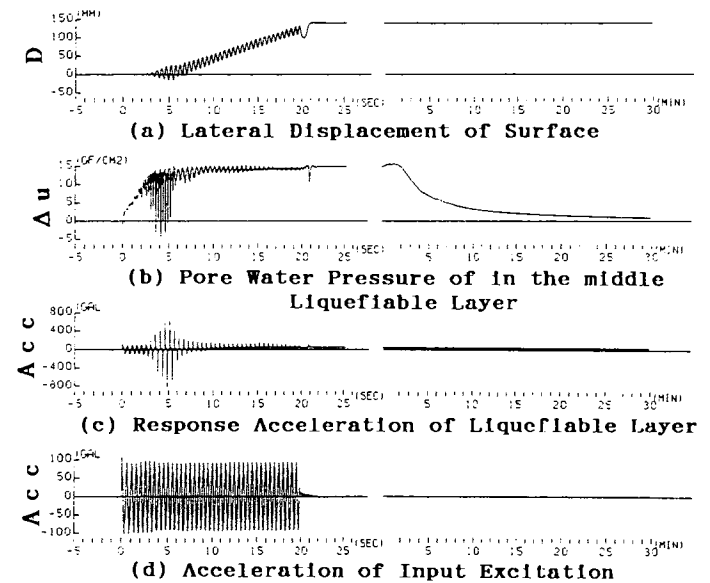

(a) Lateral Displacement of Surface

(b) Pore Water Pressure of in the middle Liquefiable Layer

(c) Response Acceleration of Liquefiable Layer

(d) Acceleration of Input Excitation

Fig. 4   Time History of Behavior of Ground (Model-6, Step-2, Section-A)

(a) Section-A

(b) Section-B
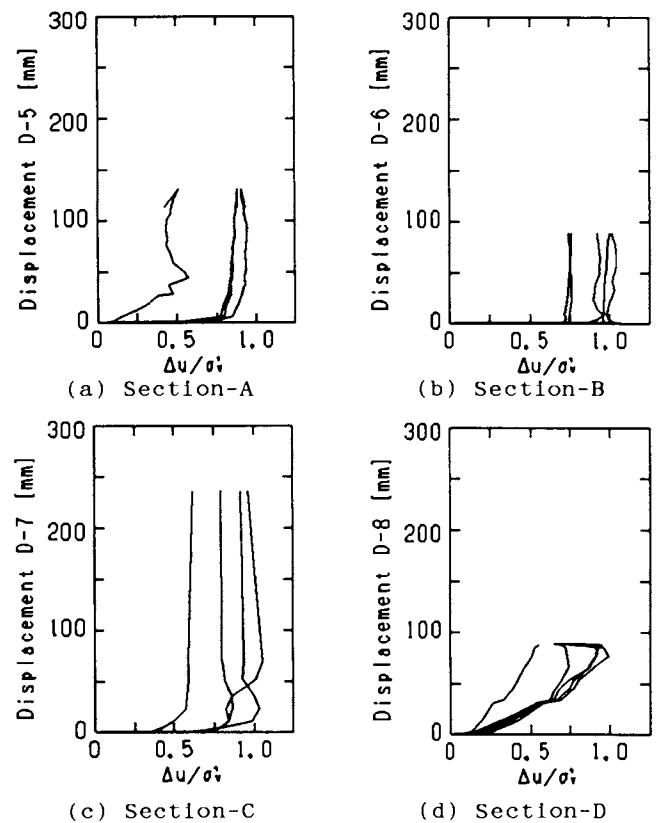
(c) Section-C

(d) Section-D

Fig. 5   Pore Water Pressure Ratio and Displacement of Surface (Model-6, Step-2: α_{max}=104gal)

267

of right-angle of excitation, respectively. Based on Figs. 7(a) and 7(b), the dynamic behavior of the pore water pressure seems similar in each layer, and the displacement at the surface seems to begin to increase at almost the same time just before the perfect liquefaction (see Fig. 4). Because the displacement meter in Fig. 7(a) is set in the direction of excitation and the one in Fig. 7(b) is set in the direction of right-angle of excitation, the displacement at the Section-OA increases vibrationally in the direction of

(a) Direction of Ground Flow

(b) Distribution of Ground Flow

Fig. 6 Directions of Ground Flow and Input Motion (Model-8, Step-2: α_{max}=94gal)

excitation and the one at the Section-OE increases gradually in the direction of right-angle of excitation. This means that the surface ground at the Section-OE is vibrated in the direction of excitation, but the ground flow occurs in the direction of slope. It can be noted that the excitation is not the cause for ground flow but that for soil liquefaction.

Judging from these characteristics concerning the ground flow, it seems that whichever the direction of excitation is, the ground flow due to soil liquefaction is induced towards the direction of slope. Because the direction of slope means that of the initial shear stress enforced by sloped overburden load, the ground seems to flow in the direction of the initial shear stress in the liquefiable layer before excitation.

Effects by Thickness of Liquefiable Layer, Surface Slope and Lower Boundary Slope

Fig. 8 compares the distribution of the lateral displacement and the lateral strains (see Fig.3) for Models-1, 3, 4 and 7, because their test conditions are similar and suitable for investigating the influence by the thickness of
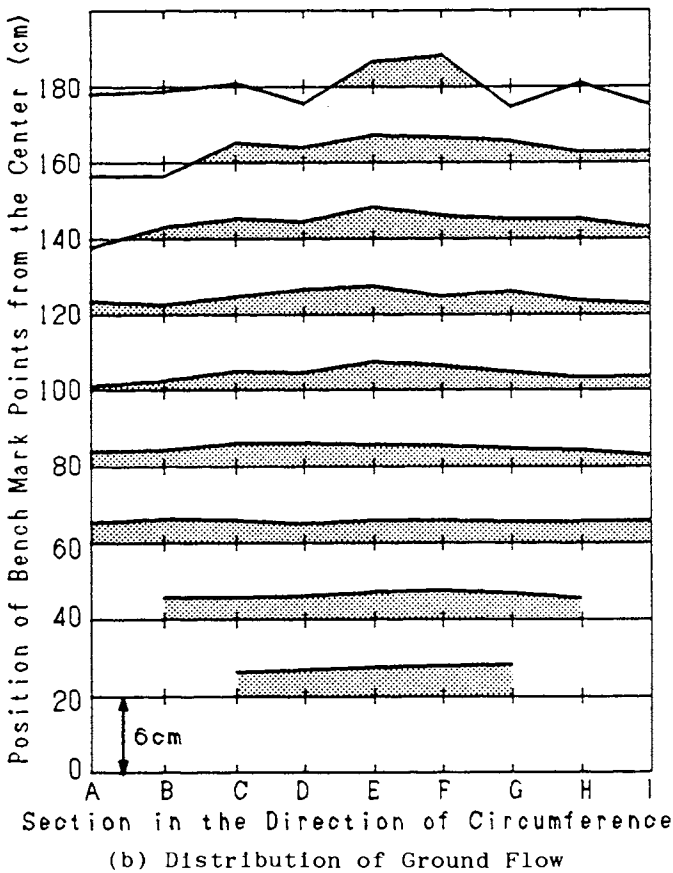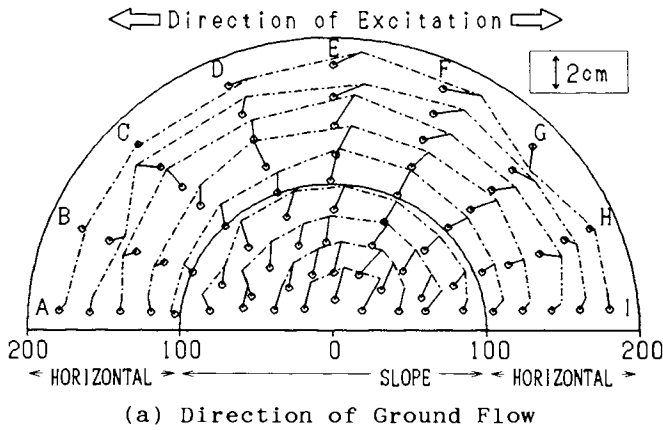

(a) Direction of Excitation (Section-OA)

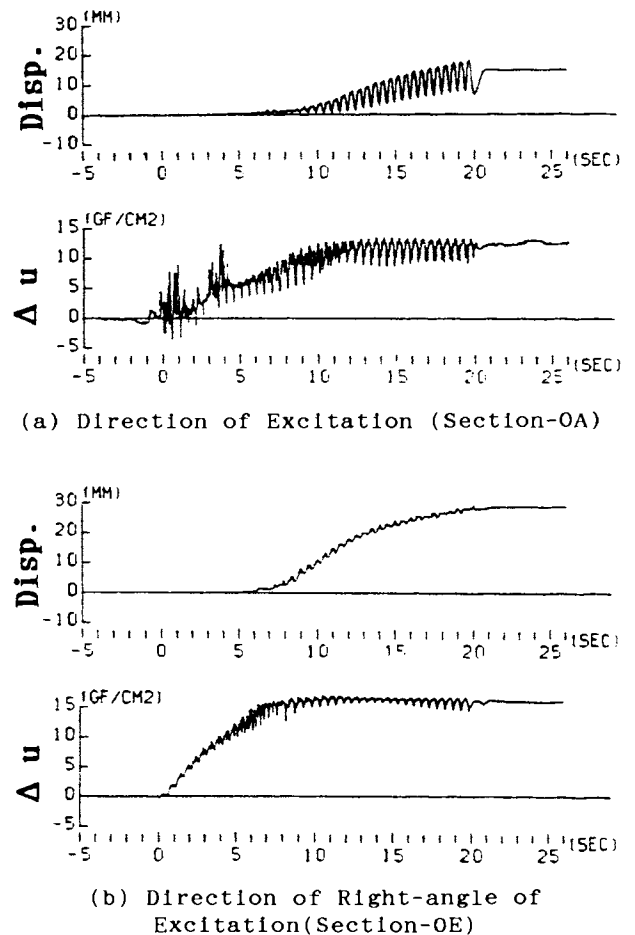(b) Direction of Right-angle of Excitation(Section-OE)

Fig. 7 Relation Between Input Motion and Lateral Displacement (Model-8, Step-1)

liqueflable layer, slopes of surface and/or lower boundary of liqueflable layer on ground flow at the surface. Comparing the results for Model-1 (θ_s= 5 %, θ_b= 0 %, H_1= 700 mm) with that for Model-4 (θ_s= 5 %, θ_b= 0 %, H_1= 350 mm), the lateral displacement and strains for Model-1 are larger than that for Model-4, and so it can be seen that the thickness of the liqueflable layer relates to the ground flow, and the displacement of ground seems to increase according to the increase of the thickness of liqueflable layer. Comparing the results for Model-3 (θ_s= 5 %, θ_b= 5 %, H_1= 350 mm) with that for Model-4, the lateral displacement and strains for Model-3 are larger than that for Model-4, and so it can be noted that the ground with both surface slope and lower boundary slope seems to be induced more than that with only surface slope. Comparing the results for Model-7 (θ_s= 0 %, θ_b= 5 %, H_1= 650 ~ 350 mm) with that for Model-1 and Model-4, the lateral displacement and strains for Model-7 are very small, and so it can be indicated that the effect of lower boundary slope by itself seems very small for the ground flow. However, comparing the results for Model-7 with that for Model-3 and Model-4, the lower boundary slope seems to become effective for the ground flow when the surface inclines.

As mentioned above, the influence of the slope of the lower boundary of liqueflable layer to the ground flow seems very small. However, when both ground surface and lower boundary of liqueflable layer incline as the case of Model-3, the slope of the lower boundary of liqueflable layer is likely to increase the ground flow.

Effects by Slope of Ground Surface

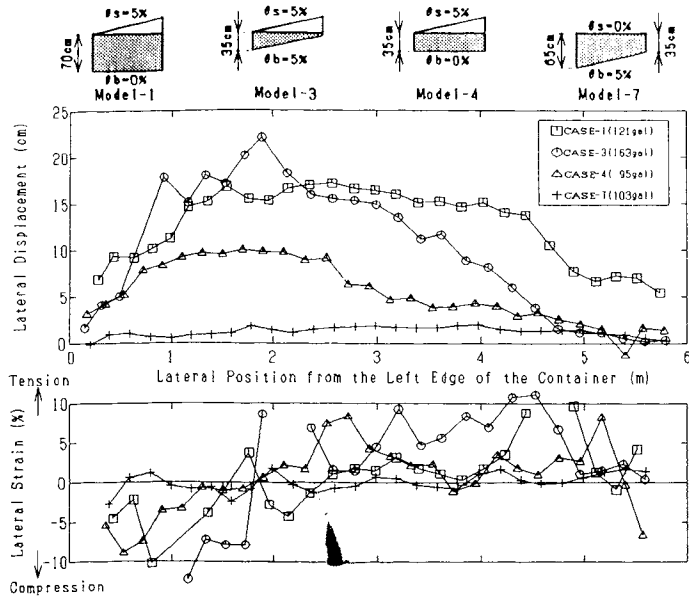Table 3 shows the typical lateral displacement measured on the ground surface at Section-B for all Models and Steps of excitation. In this Table, the ground conditions for Model-2 (θ_s= 7.5 %, θ_b= 0 %, H_1= 350 mm), Model-4 (θ_s= 5 %, θ_b= 0 %, H_1= 350 mm) and Model-5 (θ_s= 2.5 %, θ_b= 0 %, H_1= 350 mm) are similar except for the slope of ground surface. However, the shot of lead is used as the materials for Model-5, and so the slope of surface ground is converted about 10 % as sand.

Comparing the results for Models-2 and 4, it can be seen that the displacement of the ground surface seems to increase according to the increase of the surface slope, but the results for Model-5 doesn't indicate the similar tendency with Models-2 and 4. As for the cause of the difference, it can be estimated that the geotextile sheet which is set only for Model-5 between the shot of lead and the liqueflable sand layer not to mix shot of lead with sand layer, and the cables connecting the meters laid in the ground may affect the ground flow.

Estimation of Ground Flow

From the above mentioned test results, it is deduced that the slope of surface (θ_s:%) relates to the ground flow, and the ground flow seems to increase according to the increase of the surface slope (see Table 3). And the thickness of liquefied layer (H:cm) where the excess pore water pressure ratio ($\Delta u / \sigma'_v$) is almost equal to 1.0 relates to the ground flow (see Table 3, Fig. 8 and Fig. 5). Further, the duration time of excitation (T:sec) while the ratio ($\Delta u / \sigma'_v$) is almost 1.0 also relates to the ground flow (see fig. 4).

Therefore, these three parameters, i.e., θ_s, H and T can be considered as the main factors relating to the quantity of ground flow (D:cm) measured at the surface. Fig. 9 shows the relation between the parameter D/(T·H) [$*10^{-4}$ / sec] and the slope of surface (θ_s : %) at the Sections A, B, C and D at the Steps-1 and 2 for all Models excepting Model-8. The slope of surface is calculated as the average slope around the measured point on the surface at each Section. Based on this figure, it can be indicated that the parameter D/(T·H) has a tendency to increase according to the increase of the slope θ_s.
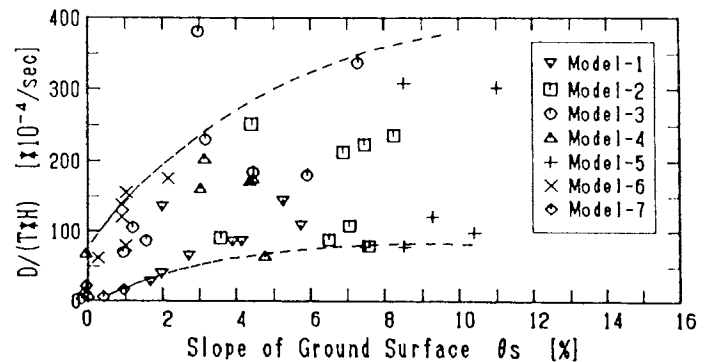

Fig. 8 Influence by Thickness and Slopes

Fig. 9 Lateral Ground Flow and Slope of Surface

269

CONCLUSION AND FUTURE RESEARCH

Based on the experimental study on the lateral ground flow due to soil liquefaction using shake table, the following can be concluded;

(1)The pore water pressure in the liquefiable layer increases firstly during excitation, preceding the lateral ground deformation, and the lateral displacement of the inclined surface begins to increase remarkably when the excess pore water pressure ratio ($\Delta u / \sigma'_v$) in the underlying layer exceeds about the range of $0.8 \sim 1.0$, and continues to increase according to the lapse of exciting time.

(2)The lateral deformation occurs only in the liquefied layers, and the unsaturated surface layer is displaced by the deformation of underlying liquefied layers.

(3)The ground seems to be deformed by shear force during excitation and the deformation mode of ground in the direction of depth differs according to the position and the lapse of exciting time.

(4)Just after stopping the excitation, the excess pore water pressure in the liquefied layer keeps the high pressure by seepage for a while and begins to decrease gradually. On the other hand, the lateral ground flow almost stops.

(5)The lateral ground flow is affected severely by the slope of ground surface, and the slope of the lower boundary of the liquefiable layer doesn't affect so much by itself, but affects when the ground surface also inclines.

(6)The direction of excitation has no significant influence to the direction of the lateral flow of ground, and the lateral ground deformation is related to the direction of the slope of surface, i.e., the direction of initial shear stress in the liquefiable layer before excitation. The excitation doesn't relate with the direct cause for ground flow but that for soil liquefaction

(7)The lateral ground flow at the ground surface (D) in this series of experiments can be expressed by the slope of surface (θ_s), the thickness of almost perfectly liquefied layer (H) and the duration time of excitation after almost complete liquefaction (T). The relation between the parameter $D/(T \cdot H)$ and θ_s can be indicated as Fig. 9.

As mentioned above, the fundamental characteristics on ground flow due to soil liquefaction

are investigated experimentally and the principal factors which cause the ground flow are clarified qualitatively.
However, it should be noted that the results are derived from the limited conditions for shake table tests and further investigation should be executed from now on.
The subjects in the future can be considered as follows:

(1)Establishment of the test conditions considering the actual site conditions during earthquakes, for example, the scale of a container, the relative density of liquefiable layer, the ground water level.

(2)Investigation of the cause of the difference between the experimental characteristics and the actual phenomena observed during earthquakes, for example, the progress of the ground flow after excitation.

(3)Investigation of the influence of ground flow on the structures, for example, pile foundations of bridges.

(4)Application of the effect of ground flow to the specifications for earthquake-resistant design.

ACKNOWLEDGEMENTS

REFERENCES

Hamada, M., Yasuda, S. and Wakamatsu,K. (1988), "Case Study on Liquefaction-Induced Ground Failures During Earthquakes in Japan", Proc. of First Japan-United States Workshop on Liquefaction, Large Ground Deformation and Their Effects on Lifeline Facilities, Tokyo.

Hamada, M., Yasuda, S., Isoyama, R. and K. Emoto (1986), "Observation of Permanent Ground Displacements Induced by Soil Liquefaction", Proc. of JSCE, No.376 / III -6, pp.211-220, (in Japanese).

Japan Road Association(1980,1990), "Part V Earthquake Resistant Design of Specifications for Highway Bridges"(in Japanese).

Sasaki,Y., Tokida, K., Matsumoto, H. and S. Saya (1990), "Experimental Study on Lateral Flow of Ground Induced by Soil Liquefaction", The Eighth Japan Earthquake Engineering Symposium 1990, Tokyo (under contribution).